UNIVERSITY OF CALIFORNIA SAN DIEGO

Developing a CRISPR-dCas9 system to study the functional roles of local mitotic histone deacetylation

A Thesis submitted in partial satisfaction of the requirements
for the degree Master of Science

in

Biology

by

Eduardo Modolo

Committee in charge:

Professor Alon Goren, Chair
Professor Lorraine Pillus, Co-Chair
Professor Cornelis Murre

2024

The Thesis of Eduardo Modolo is approved, and it is acceptable in quality and form for publication on microfilm and electronically.

University of California San Diego

2024

DEDICATION

I would like to dedicate this thesis to my parents Lucia and Egidio Modolo, thank you for all your constant love and support.

TABLE OF CONTENTS

LIST OF FIGURES

LIST OF ABBREVIATIONS

ChIP-seq	Chromatin immunoprecipitation followed by sequencing
CRISPR	Clustered Regularly Interspaced Short Palindromic Repeats
CRISPRa	CRISPR activation
CRISPRi	CRISPR inhibition
dCas9	“dead” CRISPR-associated protein 9
Dox	doxycycline
gRNA	guide RNA
HAT	histone acetyltransferase
HDAC	histone deacetylase
H3K4ac	acetylation on lysine 4 of histone 3
H3K4me3	tri-methylation on lysine 4 of histone 3
H3K27ac	acetylation on lysine 27 of histone 3
H3K9ac	acetylation on lysine 9 of histone 3
Mut	mutant
NDR	nucleosome depleted region
rlog	regularized logarithm
STC	S-trityl-l-cysteine (Kinesin 5 inhibitor)
TSS	transcription start site
WT	wild type

ACKNOWLEDGEMENTS

I would like to thank the chair of my committee, Professor Alon Goren, for his excellent mentorship and invaluable support which has helped me grow as a scientist and a person.

I would like to thank Professor Lorraine Pillus and Professor Cornelis Murre for serving on my thesis committee and offering their expertise to help my project.

I would like to thank Professor Itamar Simon, for providing helpful advice and insight to advance my work.

I would like to thank Professor Chris Benner, for the valuable assistance he provided, especially in the computational analysis portions of my research.

I would like to thank Dr. Sifeng Gu, for all the guidance he offered on molecular cloning, probably saving me months of troubleshooting.

I would like to thank Professor Eric Mendenhall, especially for his aid in CRISPR-dCas9 design and theory.

Lastly, I would like to thank all the members of the Goren Lab, especially: Dr. Lingzhi Zhang for her help in cell culture, Yuwei Cao for instruction on automated ChIP-seq, and Lauren Patel for mentoring me when I first joined the lab and providing advice and assistance on the day to day.

VITA

2023 Bachelor of Science in Molecular and Cell Biology, University of California San Diego

2024 Master of Science in Biology, University of California San Diego

ABSTRACT OF THE THESIS

Developing a CRISPR-dCas9 system to study the functional roles of local mitotic histone deacetylation

by

Eduardo Modolo

Master of Science in Biology

University of California San Diego, 2024

Professor Alon Goren, Chair
Professor Lorraine Pillus, Co-Chair

Throughout mitosis, the cell's genome is faced with drastic structural and transcriptional alterations that it must overcome to faithfully propagate its transcriptional program to the next generation. The cell most likely reestablishes the interphase chromatin organization and gene expression program after mitosis with the help of epigenetic information encoded on the mitotic

chromosomes (termed as mitotic bookmarking). A recent study comparing mitotic and interphase histone modifications discovered associations between local histone deacetylation and gene expression patterns, suggesting the acetylation state as a mitotic bookmark. This study hypothesizes that HDAC mediated, mitotic-specific, deacetylation of the nucleosome entering the TSS-associated NDR during mitosis, is bookmarking genes to reactivate earlier than others after mitosis. To test the roles of this local mitotic histone deacetylation, we would need a system that perturbs the suggested "bookmarking" deacetylation pattern in mitosis, to then measure the effects on reactivation kinetics. In this master's thesis, I am developing and evaluating the potential of a CRISPR-dCas9 system to investigate the roles of mitotic histone deacetylation patterns in the NDR on transcription reactivation regulation.

After establishing HeLa-S3 cell models expressing three different fusion proteins, VPR-dCas9 and WT/Mut p300 core-dCas9, I performed mitotic synchronization and ChIP-seq. I was able to probe chimera directed acetylation in mitotically synchronized and unsynchronized cells, looking at differences in activity when targeted to various regions in the NDR of a test gene. Across all the ChIP-seq experiments for both fusion proteins, the results displayed an interesting distinction in acetylation activity between the interphase and mitotic conditions when targeted to a certain region in the NDR of the test gene. While further research is required, my results indicate that the CRISPR-dCas9 system has the potential to specifically perturb local histone acetylation patterns both in interphase and mitosis, and serves as a viable option to study our mitotic bookmarking hypothesis.

INTRODUCTION

Throughout the complex process of cell division, many of the genomic characteristics responsible for maintaining a cell's identity are drastically altered. Transcription becomes largely repressed, RNA polymerase and many transcription factors dissociate from the mitotic chromatin, and the cell-type specific, three-dimensional genomic structure of interphase is lost (Parsons and Spencer 1997; Prasanth et al. 2003; Naumova et al. 2013). The restoration of the parent cell's transcriptional program and interphase chromatin structure in the newly formed daughter cells is thought to be assisted by epigenetic information, such as transcription factors and histone modifications, left on the chromatin during mitosis (Liu et al. 2017; Wang and Higgins 2013). This maintenance of epigenetic information on mitotic chromosomes is termed "mitotic bookmarking," and is considered to be instrumental the transmission of transcriptional memory and cell identity from the parent cell to the next generation (Palozola, Lerner, and Zaret 2019; Raccaud and Suter 2018).

Various epigenetic elements are suggested to regulate gene expression throughout mitosis. Chromatin structures such as nucleosome variants and their dynamics have been found to function in mitotic transcriptional silencing and post-mitotic reactivation of genes that are active only in interphase. The +1 nucleosome from the transcription start site (TSS), containing the H2A.Z histone variant, has been observed to shift upstream into the TSS of mitotically silenced genes during mitosis, indicating a possible regulatory mechanism (Kelly et al. 2010). Additionally, many transcription factors have been proposed as mitotic bookmarks, regulating timely transcriptional reactivation of important genes. A Transcription factor with pioneering characteristics during the zygotic genome activation of *Drosophila* early embryos, GAGA Associated Factor, is shown to stably bind mitotic chromosomes. Knockdown of this factor by

RNAi shows disturbances in transcriptional reactivation post-mitosis, asserting its importance in the timely reestablishment of the interphase expression program (Maëlle Bellec et al. 2022). Histone modifications have also been identified as mitotic bookmarks, such as the involvement of H4K5ac in propagating active chromatin states and regulating transcription reactivation, likely through its interaction with the chromatin remodeler BRD4 (R. Zhao et al. 2011). This important and growing field of mitotic memory research is essential to further the understanding of cellular processes and organismal development, as it provides insight into how cells maintain and differentiate their identity (Maelle Bellec, Radulescu, and Lagha 2018; Zaret 2014). However, there is still much to discover regarding the function of histone modifications in mitotic regulatory processes.

In effort to further understand the roles of histone modifications in the regulation of mitotic transcriptional changes, a paper published in 2018 *(Study of mitotic chromatin supports a model of bookmarking by histone modifications and reveals nucleosome deposition patterns)* by the Simon and Goren Labs, employed many techniques to compare mitotic and interphase histone modifications at global levels and spatial localization. By combining immunofluorescence, proteomics, and chromatin immunoprecipitation followed by high throughput sequencing (ChIP-seq), this study gathered data on the following histone modifications: H3K9ac, H3K27ac, H3K4me1, H3K4me3, H3K27me3, and H3K36me3. Cell populations were arrested in a metaphase-like state using a kinesin 5 inhibitor molecule S-trityl-l-cysteine (STC) (Skoufias et al. 2006), allowing comparisons to be made regarding the epigenomic landscapes of synchronized "mitotic" and unsynchronized "interphase" HeLa-S3 cells. Utilizing quantitative immunofluorescence and mass spectrometry-based approaches, they observed that global levels of histone methylations remain mostly unchanged between interphase and mitosis, while the

levels of histone acetylations showed a global decrease during mitosis. Using ChIP-seq to map localization of the histone acetylation and methylation marks, the study determined that the spatial organization of these modifications is highly similar between interphase and mitosis, with the exception of a histone deacetylation patterns near the transcription start site (TSS) of most genes (Javasky et al. 2018).

Many eukaryotic gene promoters contain a region upstream of their TSS that is free of nucleosomes, termed the "nucleosome depleted region" (NDR). These regions have been shown to contain transcription factor binding sites and are thought to assist transcription activation (Bai et al. 2010). Analysis of H3K4me3 localization with ChIP-seq to map nucleosome positioning, showed that for most genes, a methylated nucleosome enters this NDR during mitosis (Liang et al. 2015) (**Fig. 1A,B,C**). ChIP-seq for H3K9ac and H3K27ac discovered that genes can be categorized into 4 groups depending on the nucleosome occupancy and histone modifications present in their TSS-associated NDRs during interphase and mitosis (**Fig. 1A**). Group 1 (about 22% of genes) contains genes that have an NDR present at their TSS in interphase and mitosis, while Group 4 (about 8% of genes) do not contain an NDR near their TSS in either phase. Genes with a nucleosome occupying their TSS-associated NDR during mitosis can be further categorized into 2 groups based on the acetylation states of this entering nucleosome. Approximately 61% of genes have a methylated but non-acetylated nucleosome occupying their NDR during mitosis (labeled as Group 2 genes), while about 9% of genes contain a methylated and acetylated nucleosome in this position (labeled as Group 3 genes) (**Fig. 1A,B,C**). Potential contributors to this acetylation pattern were investigated, examining ChIP-seq data of histone deacetylases (HDACs) from unsynchronized cells. This analysis revealed that HDAC peaks were present at 43% of the Group 2 gene TSSs, but only at 35% of Group 3 gene TSSs. Additionally, treatment of HeLa-S3 cells

with the pan-HDACs inhibitor TSA counteracted the pattern of deacetylated nucleosomes in the NDR during mitosis (**Fig. 1E**) Combined, these findings form a hypothesis that the nucleosome entering the NDR of Group 2 genes during mitosis is being particularly deacetylated by HDACs.

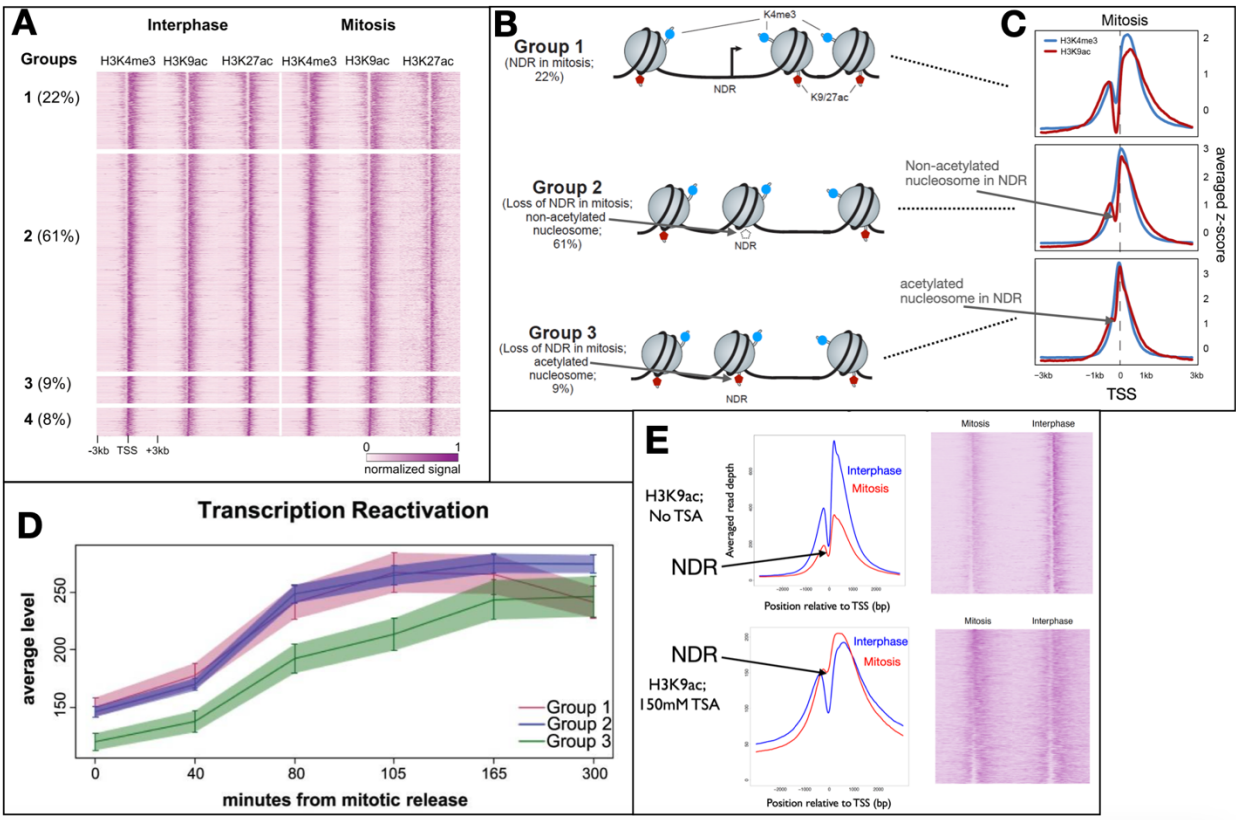

Figure 1. Classification and analysis of histone modification patterns in TSS-associated NDRs.

Panels A and D adapted from Javasky et al. 2018. **A)** Heatmap of 5731 genes ranging 3kb up and downstream from the TSS showing normalized and standardized Z-scores for histone modifications: H3K4me3, H3K9ac, and H3K27ac in interphase and mitosis. The four gene groups were separated manually. **B)** Schematic of histone modifications present at the NDR during mitosis for Groups 1-3. **C)** Metagene plots displaying the average signal of each histone modification around the TSSs of the 3 groups of genes in mitosis. **D)** Average transcription level at different time points after mitotic release for gene Groups 1-3. **E)** Metagene plot and heatmap showing average H3K9ac signal around the TSS for interphase and mitotic cells, treated or untreated with the HDAC inhibitor TSA.

To discover the possible regulatory roles of the mitotic histone deacetylation patterns observed in the NDR of most genes, the post-mitotic transcription reactivation rates as well as

Gene Ontology (GO) of each gene group were analyzed. Transcription reactivation kinetics determined that genes in Groups 1 and 2 reactivated significantly faster than Group 3. This analysis was done using the data collected in (Palozola et al. 2017), which used EU-RNA-seq in HUH7 human hepatoma cells to map nascent transcription at different time points after release from nocodazole-induced mitotic arrest. A collection of cell cycle genes (Whitfield et al. 2002), housekeeping and tissue-specific genes (https://www.proteinatlas.org/), as well in genes transcribed in HeLa-S3 cells (Hart et al. 2013) was curated. Using the Palozola reactivation data, the average transcription level for each gene Group (1-3) at different time points after mitotic release was plotted (**Fig. 1D**).

Gene Ontology analysis concluded that genes in Groups 1 and 2 are significantly enriched for functions such as RNA processing, cell adhesion, and signal transduction, which could potentially be more important directly following mitotic exit. Taken together, these associations add to the previously discussed hypothesis, suggesting that the HDAC mediated, mitotic-specific, deacetylation of the nucleosome entering the NDR during mitosis is functioning to bookmark genes that have more important roles directly following mitotic exit.

A potential mechanism for this deacetylation dependent bookmark could be through the interaction of acetylated histones with chromatin remodeling complexes, specifically those containing an acetyl-lysine binding bromodomain (Swygert and Peterson 2014). Previous studies suggest that acetylated histones stabilize the binding of chromatin remodelers to the nucleosome, as seen in the increased retention of the remodeling complex SWI/SNF on acetylated promoter nucleosomes (A. H. Hassan, Neely, and Workman 2001; Ahmed H. Hassan et al. 2002). Perhaps the deacetylation of the nucleosome entering the NDR during mitosis serves the purpose of altering interactions with chromatin remodeling enzymes, resulting in earlier reestablishment of the NDR

and transcription reactivation after mitotic exit. Of course, there are many factors that determine nucleosome stability and positioning (Struhl and Segal 2013) and this hypothetical explanation requires further investigation.

One method of testing hypothesized mitotic bookmarks is to experimentally perturb the bookmark to then monitor the effects on gene reactivation post mitosis. However, due to the local functionality and temporal nature of these epigenetic elements, there is a current lack of molecular tools to locally modify bookmarks specifically during mitosis. This makes it very difficult to study the explicit roles of these epigenetic elements (Raccaud and Suter 2018; Festuccia et al. 2017). As seen in the 2018 paper by the Simon Lab, small molecules can be used to inhibit HDACs and perturb the NDR acetylation patterns in mitosis, however a drawback to this approach is the off-target effects of globally inhibiting HDAC activity. Another approach would be to recruit histone acetyltransferases (HATs) and HDACs directly to the NDR, to modify the local levels of histone acetylation during mitosis. Utilizing CRISPR-dCas9 (Clustered Regularly Interspaced Short Palindromic Repeats and endonuclease "dead" CRISPR-associated protein 9) to carry HATs and HDACs to targeted loci could be a potential method to examine our mitotic bookmarking hypothesis.

In this master's thesis, I am evaluating a CRISPR-dCas9 system for its potential to investigate the roles of local mitotic histone deacetylation patterns on transcription reactivation regulation. Using a multitude of cloning techniques, I established plasmid constructs containing either a VPR-dCas9 or a wild type or mutant p300 core-dCas9 fusion protein. I used these constructs along with a custom gRNA donor plasmid, to generate stable HeLa-S3 cell lines expressing different combinations of dCas9 fusion protein and gRNA, targeting various regions of the NDR of a test gene. With mitotic synchronization and ChIP-seq, I observed fusion protein

directed acetylation increases in interphase and mitosis. The results suggested that dCas9 fusion protein acetylation activity depends on both the targeted position in the NDR and the synchronization condition. Interestingly, when targeted to 100bp upstream of the TSS of our test gene, all acetylation causing fusion proteins appeared to only increase acetylation in mitosis. Future research is required to explain this observation; however, it may suggest a method to achieve the mitotic-specific perturbation of NDR acetylation levels that is required to test our mitotic bookmarking hypothesis.

Chapter 1 MATERIALS AND METHODS

Hela-S3 cell culture

HeLa-S3 cells from ATCC (CCL-2.2) were cultured in Gibco™ DMEM, high glucose (Thermo Fisher Scientific cat. 11-965-118) with 10% Heat inactivated FBS (Life Technologies cat. 10438026), 1% Gibco™ Antibiotic-Antimycotic (Thermo Scientific cat. 15240062), and 1% sodium pyruvate (Gibco cat. 11360070), grown at 37 C and 5% CO2.

Cloning Plasmid Constructs:

VPR-dCas9:

Started with plasmid *PiggyBac dCas9-VPR* (Addgene #191269). This plasmid contained the puromycin resistance marker, however the plasmid carrying the gRNA cassette: *PB-U6insert-EF1puro* (Addgene #104537) (Goren Lab ID bGG298), already provides puromycin resistance. Therefore, the first cloning step was to replace the puromycin resistance sequence in the *PiggyBac dCas9-VPR* plasmid with the hygromycin B resistance sequence (gift from Dr. Sifeng Gu). This was done by digesting the *PiggyBac dCas9-VPR* plasmid with MfeI-HF and HpaI and gel extracting the linearized plasmid to remove the puromycin sequence. NEBuilder® HiFi DNA Assembly (NEB cat. E2621S) was then performed to insert the hygromycin B sequence, amplified from Dr. Gu's plasmid with GoTaq Green PCR master mix (Promega cat. PRM7123) in the place of the puromycin sequence. The new plasmid was called *PB_VPR-dCas9-BFP_hygro*, noted as *VPR-dCas9* in **Fig. 2A** (Goren Lab ID bGG296).

WT/Mut p300 core-dCas9:

Primer mutagenesis in conjunction with NEBuilder® HiFi DNA Assembly was used to remove the BspQI (type II restriction enzyme) cut site from the *PB_VPR-dCas9-BFP_hygro*

plasmid to prepare for future cloning steps. Additionally, the BFP reporter gene sequence was swapped for that of enhanced GFP (EGFP) (amplified from *pGL3-U6-sgRNA-EGFP* Addgene #107721) to make validation of fusion protein expression easier to visualize. This new plasmid was called *PB_VPR-dCas9-EGFP_hygro* (Goren Lab ID bGG312). Next, the VPR region was removed from this new plasmid by digesting with AgeI-HF and BglII, and a gBlock (ordered from IDT) was inserted upstream of the dCas9 sequence in place of the extracted VPR sequence. This gBlock contained a BspQI Golden Gate cloning site followed by a glycine and serine rich linker sequence (linker sequence was copied from *p300 core-dCas9-p300 core* Addgene #179557). This new plasmid: *PB_GG-linker-dCas9-EGFP_hygro* (Goren Lab ID bGG326), provided a backbone dCas9 plasmid with a Golden Gate cut site and linker upstream of the dCas9 where I could insert the WT and Mut p300 core sequences using Gibson Assembly. The WT and Mut p300 core sequences were amplified from *pcDNA-dCas9-p300 core* (Plasmid #61357) and *pcDNA-dCas9-p300 (D1399Y)* (Plasmid #61358) respectively and inserted into the Golden Gate cut site after digestion with BspQI. These new plasmids were named: *PB_p300_core-dCas9-EGFP_hygro* and *PB_Mut_p300_core-dCas9-EGFP_hygro*, labeled *WT p300 core-dCas9* and *Mut p300 core-dCas9* on **Fig. 2A** (Goren Lab ID bGG327 and bGG328 respectively).

Cloning gRNA donor plasmid:

I started with plasmid: *PB-U6insert-EF1puro* (Addgene #104537) and digested with EcoR1-HF and Age1-HF followed by gel extraction. This created a gap downstream of the U6 promoter where I inserted a gBlock using T4 DNA ligase (NEB cat. M0202L). This gBlock contained a BbsI Golden Gate cloning site directly upstream of the S. Pyogenes sgRNA scaffold sequence. This new plasmid, called the *PB_SPscaffold_BB* (Goren Lab ID bGG298), served as a backbone in which to clone in our custom sgRNA protospacers using the BbsI Golden Gate site

upstream of the S. Pyogenes scaffold sequence. Next, we digested the *PB_SPscaffold_BB* plasmid with BbsI-HF and gel extracted the backbone, then ligated our custom protospacers (targeting our gene of interest) into the Golden Gate site. These final plasmids served as our *gRNA donor* plasmids, shown in **Fig. 2A(*iv*)**. Validation of protospacer insertion was done with PCR.

Ordering guide RNA protospacers:

Protospacers were ordered from IDT as top and bottom oligos with overhangs for the Golden Gate BbsI cut sites and annealed together before ligation into the *PB_SPscaffold_BB* plasmid. I utilized the CRISPR tool on Benchling to generate potential protospacers and chose the sequences with the highest On-Target Score that were within our desired ranges from the TSS.

Transfection and selection protocol:

All transfections were done with a 24 well plate using Lipofectamine™ 3000 Transfection Reagent (ThermoFisher Scientific, Cat: L3000015). The day before the transfection, 100k cells were seeded on the 24 well plate. The piggyBac plasmid carrying the dCas9 fusion protein cargo was cotransfected alongside the plasmid expressing the transposase enzyme (gift from Dr. Sifeng Gu, pCSJ533**)** into HeLa-S3 cells. In total 1ug of DNA was transfected, using equimolar cargo plasmid and transposase plasmid (666ng of fusion protein plasmid, 333ng of transposase plasmid). About 48-72 hours after transfection with lipofectamine, selection was started using 400 ug/ml of hygromycin B (Invitrogen cat. 10687010) for 10 days, refreshing the media and hygromycin every other day. Expression of VPR-dCas9 was validated through BFP fluorescence, while expression of the WT/Mut p300 core-dCas9 was validated through EGFP fluorescence. After piggyBac integration of the fusion protein was complete, the *gRNA donor* plasmid was cotransfected into each fusion protein cell line with the transposase plasmid using Lipofectamine™ 3000

Transfection Reagent. Equimolar *gRNA donor* plasmid to transposase plasmid was used. Selection was performed with 0.2ug/ml puromycin (Invitrogen cat. A1113803) for 5 days. Validation of gRNA expression was done through reverse-transcription PCR (RT-PCR) (SuperScript™ II Reverse Transcriptase cat. 18064014). After selection with puromycin, another round of selection with hygromycin was performed to make sure the gRNA cargo transposition did not disrupt any of the dCas9 cargo transposons.

Dox Induction and Mitotic synchronization

Mitotic synchronization protocol used from (Javasky et al. 2018) in the Cell culture and synchronization section of Methods. Expression of the fusion protein was induced in each of the cell lines (each grown in a 10cm mammalian cell culture dishes) by adding doxycycline (Sigma-Aldrich D9891-1G) at 2ug/ml for 4 days (replacing the media with fresh dox on day 2 of the 4-day treatment). On the 4th day the cells were pre-synchronized in G1/S by addition of 2 mM thymidine for 16 h. After 16 hours, the cells were washed with PBS and released for 3 h in fresh medium. Next, 10μM S-trityl-L-cysteine (STC) mixed with medium was added to the cells and incubated for 12 h. After 12 hours the cells were fixed and harvested for ChIP-seq.

Double Cross-linking Fixation and ChIP-seq

Followed the protocol from *An optimized protocol for rapid, sensitive and robust on-bead ChIP-seq from primary cell*s (Texari et al. 2021). ChIP-seq protocol was done either manually or using automation with the liquid handler machine: “Bravo” (Agilent model 16050-102).

Protocol Overview:

Roughly 10 million cells per sample were fixed by double crosslinking with disuccinimidyl glutarate (DSG) (CovaChem cat. 13301-5x100) and Formaldehyde (Pierce- ThermoFisher cat. PI28906). Cells were then lysed, and chromatin was sheared using a PIXUL Multi-Sample Sonicator. Whole cell extract was de-crosslinked and cleaned to use as input DNA, and immunoprecipitation (IP) was done by incubating sheared chromatin with an antibody specific to our desired epitope and then washing away the background chromatin. Final IP and Input libraries were prepared using the NEBNext® Ultra™ II DNA Library Prep Kit for Illumina® (cat. E7645S) and dual and single barcoded adapters from NEXTflex were used. Antibodies used: Acetyl Histone H3 (Lys9) (C5B11) Rabbit mAb (Cell Signaling Technology cat. 9649S) and Acetyl-Histone H3 (Lys27) (D5E4) XP® Rabbit mAb (H3K27ac) (Cell Signaling Technology cat. 8173S)

Bioinformatics Analysis:

My ChIP-seq libraries were sequenced using Illumina's NextSeq 500/550 High Output Kit v2 (75 cycles) cat. 20024906. Adaptor sequences were trimmed using Trimmomatic (Bolger, Lohse, and Usadel 2014) and then FastQC (Andrews 2010) was performed on the trimmed fastq files for quality assurance. Fastq files were then aligned to the hg38 genome using BWA (Li and Durbin 2009), and the sam files were converted to bam and processed, removing duplicate reads, using Samtools (https://www.htslib.org/doc/samtools.html). Tag directories were made using HOMER (Heinz et al. 2010) (http://homer.ucsd.edu/homer/) with fragment length set to 150. Read depth normalized bigWigs were made with HOMER's command: makeBigWig.pl, which uses the UCSC program bedGraphToBigWig (Kent et al. 2010).

To generate regularized log (rlog) transformed bigWigs, tag counts in 50bp bins, 200kb up and downstream of the PRCC NDR, were counted using the annotatePeaks.pl command from

homer, with the -raw and -rlog options set (the rlog transformation is from the DESeq2 package). The tag counts for this region were then turned into bedgraphs, then bigWigs. Next, rlog normalized bigWigs for each treatment condition were subtracted by rlog normalized bigWigs for the appropriate control condition using bigwigCompare from deepTools. All bigWigs were visualized on the UCSC genome browser (Nassar et al. 2023). The read depth normalized, the log transformed, and the rlog transformed scatter plots were plotted using ggplot2 in R. The data was calculated by using HOMER's annotatePeaks.pl on tag counts in 1kb bins for the entire chromosome 1, using default for read depth normalized, -log for log transformed, and -raw -rlog options of the rlog transformed scatter plots.

Chapter 2 RESULTS

Chapter 2.1 Establishing CRISPR-dCas9 system in HeLa-S3 cell model

CRISPR-dCas9 Fundamentals:

For CRISPR-dCas9 systems to function, each cell must contain two essential components: a guide RNA (gRNA) and the dCas9 protein often fused to an effector enzyme domain. The gRNA is an RNA molecule containing a protospacer and scaffold sequence. The scaffold sequence folds into a stem and loop structure that complexes with the dCas9 protein, while the protospacer provides the specific ~20bp nucleotide sequence complementary to the genomic target loci. The dCas9, once associated with the gRNA, can then scan the genome and search for the sequence complementary to the protospacer. If the sequence appears next to a proper protospacer adjacent motif (PAM), the dCas9 enzyme can bind to this locus (Qi et al. 2013).

The CRISPR-dCas9 differs from the traditional CRISPR-Cas9 system in that the dCas9 is mutated to no longer have endonuclease activity (hence the name "dead Cas9"), and therefore only functions in the localization to targeted loci. Since its development in 2013, the CRISPR-dCas9 system has been used in many techniques to modify epigenetic landscapes and regulate gene expression. Fusing the dCas9 protein to a transcriptional repressor domain such as the Krüppel-associated box (KRAB), yields a tool for CRISPR transcriptional inhibition (CRISPRi). Linking the dCas9 protein to a transcriptional activator domain such as VP64 (a tetramer of VP16, the herpes simplex virus protein 16) creates a CRISPR transcriptional activation tool (CRISPRa) (Kampmann 2018; Qi et al. 2013; Karlson et al. 2021). To probe the possibilities and limitations of a CRISPR-dCas9 system to target TSS-associated NDRs and locally modify the mitotic histone acetylation patterns, I generated HeLa-S3 cells expressing the CRISPR-dCas9 components,

synchronized these cells in mitosis, and performed ChIP-seq for histone acetylations to observe the behavior of the fusion protein system.

Generating HeLa-S3 cell model:

A pilot fusion protein plasmid construct containing our desired elements: **1)** piggyBac integration, **2)** dox inducibility **3)** fluorescence protein reporter, **4)** antibiotic selection marker, **5)** histone acetylation capabilities of the chimera, was chosen to establish our transfection and ChIP-seq protocols (**Fig. 2A**). To make the process of genomically integrating the elements of the CRISPR-dCas9 system into our HeLa-S3 cells fast and simple, we opted to utilize a piggyBac transposon system. With this approach, plasmid constructs contain a cargo cassette flanked by inverted terminal repeats (ITRs); the entire cassette is cut out by the transposase enzyme and inserted into TTAA sites in the cell's genome (S. Zhao et al. 2016) (**Fig. 2B**). We also decided on a doxycycline (dox) inducible fusion protein expression, to potentially alleviate some collateral effects of constant dCas9 fusion protein presence, allowing us to induce expression only 4-5 days before harvest. Blue fluorescence protein (BFP) connected to the fusion protein by a P2A cleavage site, allowed for quick validation of fusion protein expression. Puromycin (later switched to hygromycin) allowed for selection of cells with integrated piggyBac cargo cassette.

This pilot fusion protein plasmid was used by the Wysoka Lab in their 2018 paper *Systematic perturbation of retroviral LTRs reveals widespread long-range effects on human gene regulation* (Fuentes, Swigut, and Wysocka 2018), and contains the VPR-dCas9 chimera (**Fig. 2A(*i*)**). The VPR, commonly fused to dCas9 in CRISPRa constructs, is a powerful transcriptional activator composed of three activation domains fused together: VP64 (discussed earlier), p65 (activation domains of NFκB subunit), and Rta (R transactivator from the Epstein-Barr virus) (Kampmann 2018). The VP64 recruits endogenous HATs such as p300 (Hilton et al. 2015) and

therefore causes high levels of histone acetylation, making the VPR-dCas9 a robust framework to test and refine our protocols for stable cell line generation and data collection with ChIP-seq.

After the VPR-dCas9 system was established and tested using ChIP-seq, I used a variety of cloning techniques to modify the fusion protein plasmid construct and insert either the wild type (WT) or a mutant (Mut) catalytic core of the p300 HAT enzyme in place of the VPR (**Fig 2A(*ii-iii*)**). The p300 core contains the bromodomain, the CH2 domain, and the HAT domain (Delvecchio et al. 2013). The bromodomain, as described previously in the context of chromatin regulators, has a similar function in the p300 core. It stabilizes interaction with the nucleosome and binds the histone substrate, allowing the HAT domain to acetylate histone residues (Manning et al. 2001). The CH2 domain stabilizes the bromodomain (Park et al. 2013). The WT and Mut sequences were obtained from the plasmids used in the study *Epigenome editing by a CRISPR/Cas9-based acetyltransferase activates genes from promoters and enhancers* (Hilton et al. 2015).

Unlike the VPR or the full length p300, which has many domains interacting with a multitude of transcription factors causing a plethora of activation effects, the p300 core should offer limited impact beyond the desired increase in histone acetylation, allowing us to study more explicitly the roles of histone acetylation (Chen and Li 2011). Additionally, we are utilizing a mutant p300 core containing a single mutated amino acid in the HAT domain, deactivating the acetyltransferase activity. This will provide our fusion protein system with a control for steric effects, additional p300 core enzymatic activities, and other confounding effects of targeting the dCas9 chimera to the NDR region. With the WT and Mut versions of the CRISPR-dCas9 tools, we can be more confident that any effects we see on transcription reactivation of targeted genes, is due to the directed perturbation of acetylation state.

To investigate dCas9 chimera behavior when targeted to different locations across the NDR, we chose a test gene: PRCC (**Fig 2. F,G**). Because we are using fusion proteins that *cause* histone acetylation, we chose a gene from Group 2 with a *non*-acetylated nucleosome entering the TSS-associated NDR during mitosis, hoping to perturb this nucleosome's deacetylated state. Protospacers were designed targeting 100bp, 350bp, and 400bp *upstream* from the TSS (also denoted as -100, -350, and -400 bp *from* the TSS). These protospacers were cloned into our gRNA backbone plasmid generating a gRNA donor plasmid (**Fig 2A(*iv*)**), and piggyBac integration was used to insert the gRNA cassette into the HeLa-S3 genomes. One cell line per gRNA target was generated, to differentiate between fusion protein activity when targeted to different distances from the TSS (**Fig. 2F**). Once the dCas9 fusion protein and gRNA cassettes were integrated into our HeLa-S3 genomes and dox induction of the chimera was validated through fluorescence proteins (**Fig 2C,D**), a subset of the cells was synchronized in a metaphase like state using STC following the same protocol as the Simon and Goren Lab paper (**Fig. 2E**). The unsynchronized and mitotically arrested cell lines targeting various locations across the NDR of PRCC, allows us to compare fusion protein acetylation activity depending on the cell phase condition and targeted locus. Fusion protein behaviors being assessed included: whether acetylation enrichment was increased, effect range, and location of increased enrichment.

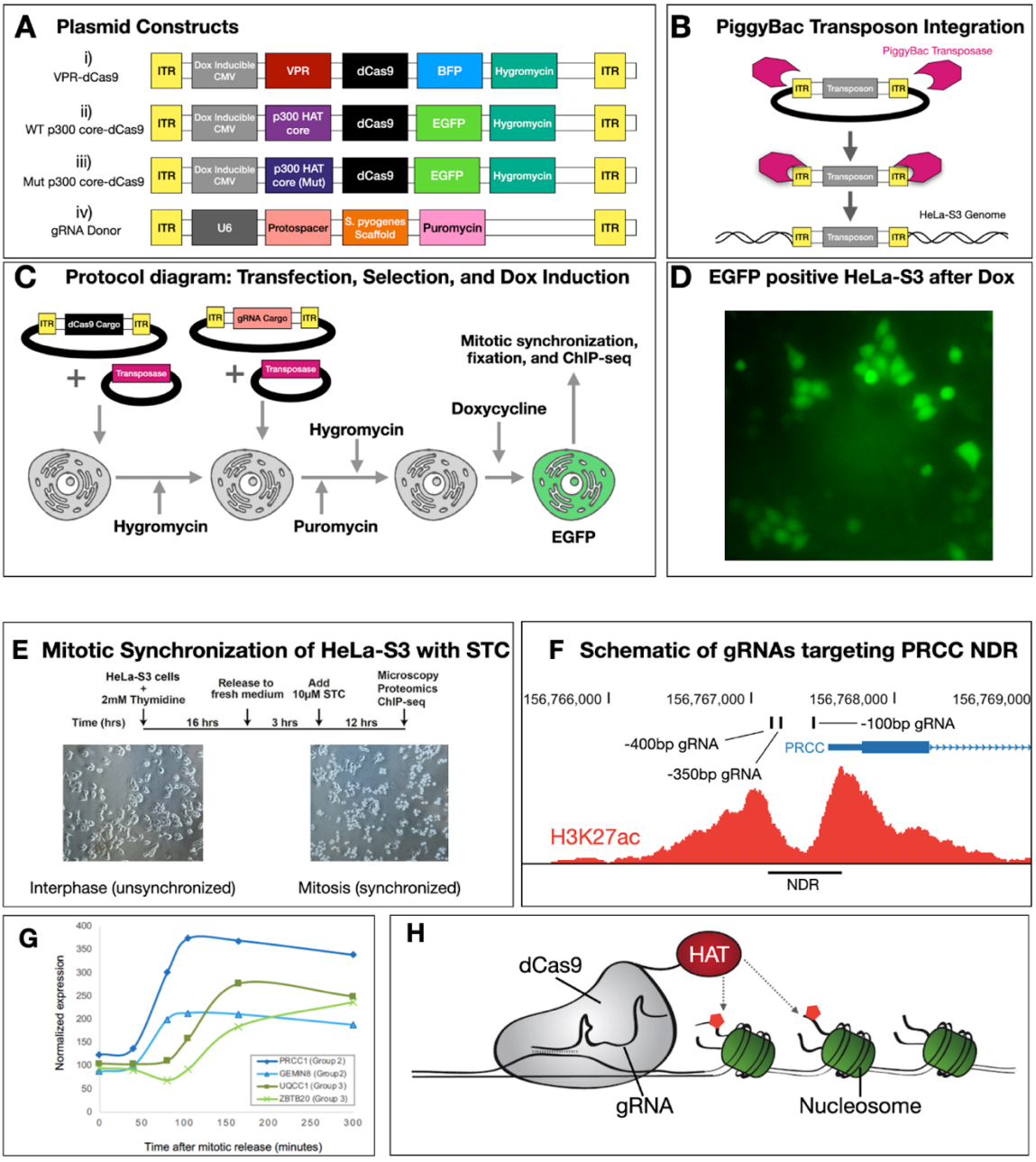

Figure 2. Establishing CRISPR-dCas9 system in HeLa-S3 cell model

A) Layout of dCas9 fusion protein and gRNA donor plasmid constructs. **B)** Illustration of the piggyBac integration method used to generate stable cell lines. **C)** Diagram of the protocol used to generate stable cell lines followed by the induction of fusion protein expression with doxycycline. **D)** HeLa-S3 cells with p300 core-dCas9 fusion protein expression validated by EGFP reporter gene. **E)** Mitotic synchronization using kinesin 5 inhibitor (STC). **F)** Schematic of gRNA target loci in the NDR region of PRCC promoter. **G)** Transcription reactivation kinetics of sample Group 2 and 3 genes, using (Palozola et al. 2017) data. **H)** Illustration of dCas9-HAT fusion protein causing histone acetylation, image adapted from (Genga, Kearns, and Maehr 2016).

Cloning Process: dCas9 Fusion protein and gRNA donor constructs:

In the process of establishing HeLa-S3 cell models expressing the components of our CRISPR-dCas9 system, I utilized multiple techniques to optimize and generate the plasmid constructs necessary. Utilizing PCR, restriction digests, gel electrophoresis, and whole plasmid sequencing, I was able to troubleshoot and validate each cloning step.

For the fusion protein constructs, I started off with a VPR-dCas9 on a piggyBac plasmid within a transposon cassette containing a BFP fluorescence reporter gene and a puromycin (puro) selection marker. The gRNA donor piggyBac plasmid already contained puromycin resistance, therefore I used restriction enzymes to remove this gene from the VPR-dCas9 plasmid and the Gibson Assembly (Gibson et al. 2009) method to insert a PCR amplified hygromycin (hygro) resistance gene in place of the puromycin (**Fig. 3A**).

Next, we noticed that the BFP was difficult to detect using our microscopes, so I PCR amplified the entire plasmid in fragments, swapping the BFP fragment for a fragment containing EGFP, and then using Gibson Assembly once again to reconstruct the plasmid. The EGFP provided better validation of dox induced expression of the fusion protein (**Fig. 3B**).

In the process of amplifying the plasmid in fragments, I used the PCR primers to perform site directed mutagenesis, removing a restriction enzyme recognition site to prepare the plasmid for future cloning. (Removal of this restriction enzyme recognition site was required for construction of the backbone dCas9 plasmid) (**Fig. 3B**).

After testing the VPR-dCas9 system, we wanted to modify our fusion protein to contain either a wild type or mutant version of the p300 core fused to the dCas9 instead of the VPR. In anticipation of future modification of effector enzymes in my plasmid, I wanted to create a

backbone dCas9 plasmid with a primed cloning site upstream of the dCas9. Using restriction enzymes, I removed the VPR sequence from upstream of the dCas9 and inserted a custom DNA fragment (gBlock ordered from IDT) containing a Golden Gate cloning (Engler and Marillonnet 2014) site made with two adjacent type IIS restriction enzyme recognition sites. This gBlock also contained a glycine and serine rich linker sequence in between the Golden Gate cloning site and the dCas9, optimized for fusing the p300 core to the dCas9 (**Fig. 3C**). Next, I PCR amplified the WT and Mut p300 core sequences from a donor plasmid and inserted them upstream of the linker and dCas9 sequence in my backbone, using the Golden Gate cloning site and Gibson Assembly (**Fig. 3D**).

The gRNA donor plasmid started with a piggyBac plasmid with only a U6 promoter and Puromycin resistance in the transposon cassette. I ordered a custom gBlock containing a Golden Gate cloning site upstream of a gRNA scaffold sequence compatible with the S. Pyogenes dCas9 protein we are using (**Fig. 3E**). After inserting this gBlock downstream of the U6 promoter, I had a backbone gRNA donor plasmid in which I could insert custom protospacers using simple Golden Gate cloning (**Fig. 3F**).

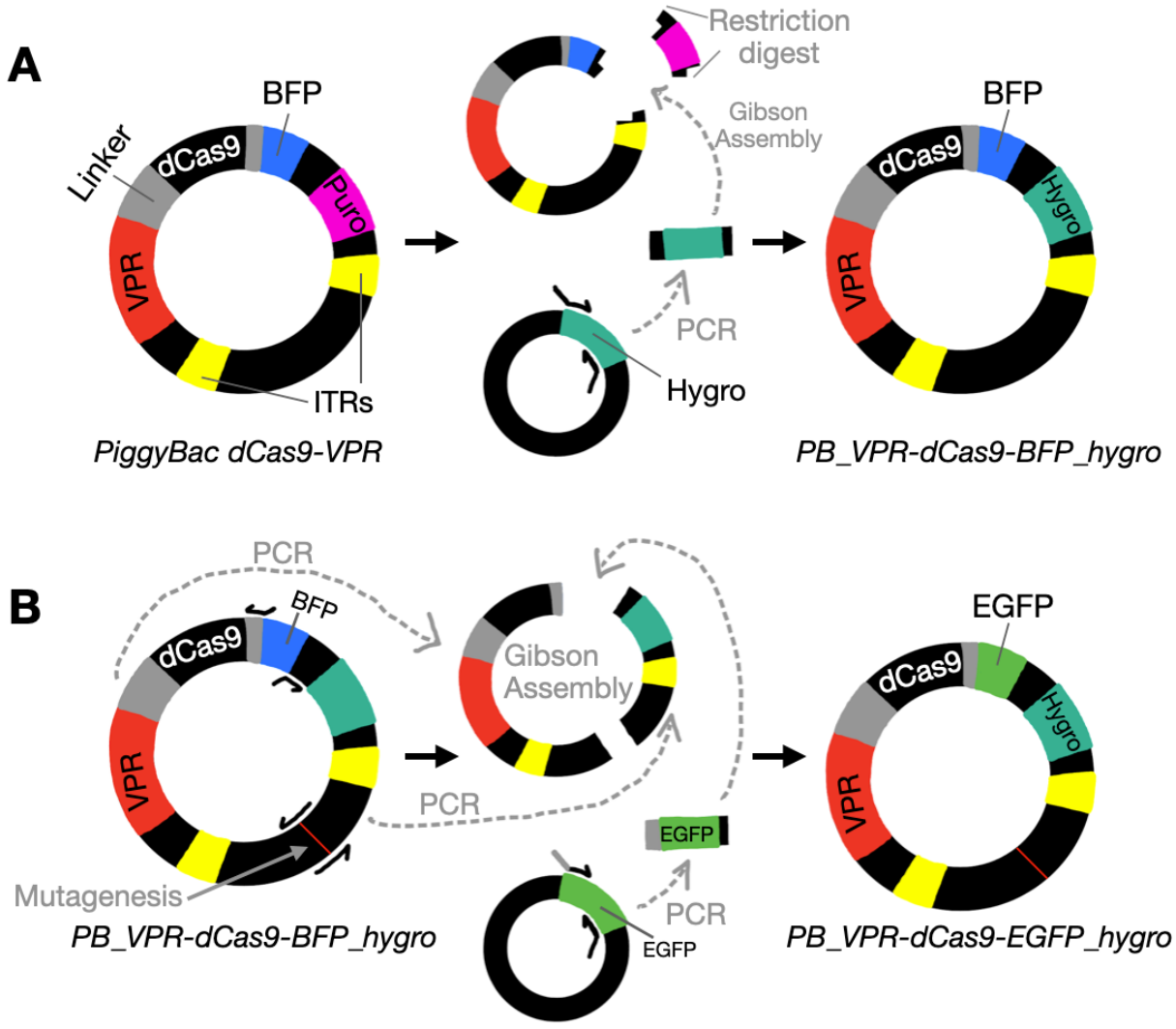

Figure 3. Cloning Procedures for dCas9 fusion protein and gRNA donor constructs.

A) Swapping puromycin selection marker for that of hygromycin in *PiggyBac dCas9-VPR.* **B)** Exchanging the BFP fluorescence reporter for EGFP. **C)** Inserting Golden Gate cloning site and linker upstream of the dCas9. **D)** Inserting the p300 core sequence upstream of the linker and dCas9 to make the complete p300 core-dCas9 fusion protein. **E)** Insertion of Golden Gate site and S. Pyogenes gRNA scaffold into the *PB-U6insert-EF1puro* plasmid. **F)** Ligation of gRNA protospacer into the Golden Gate cut site to generate complete gRNA donor plasmid.

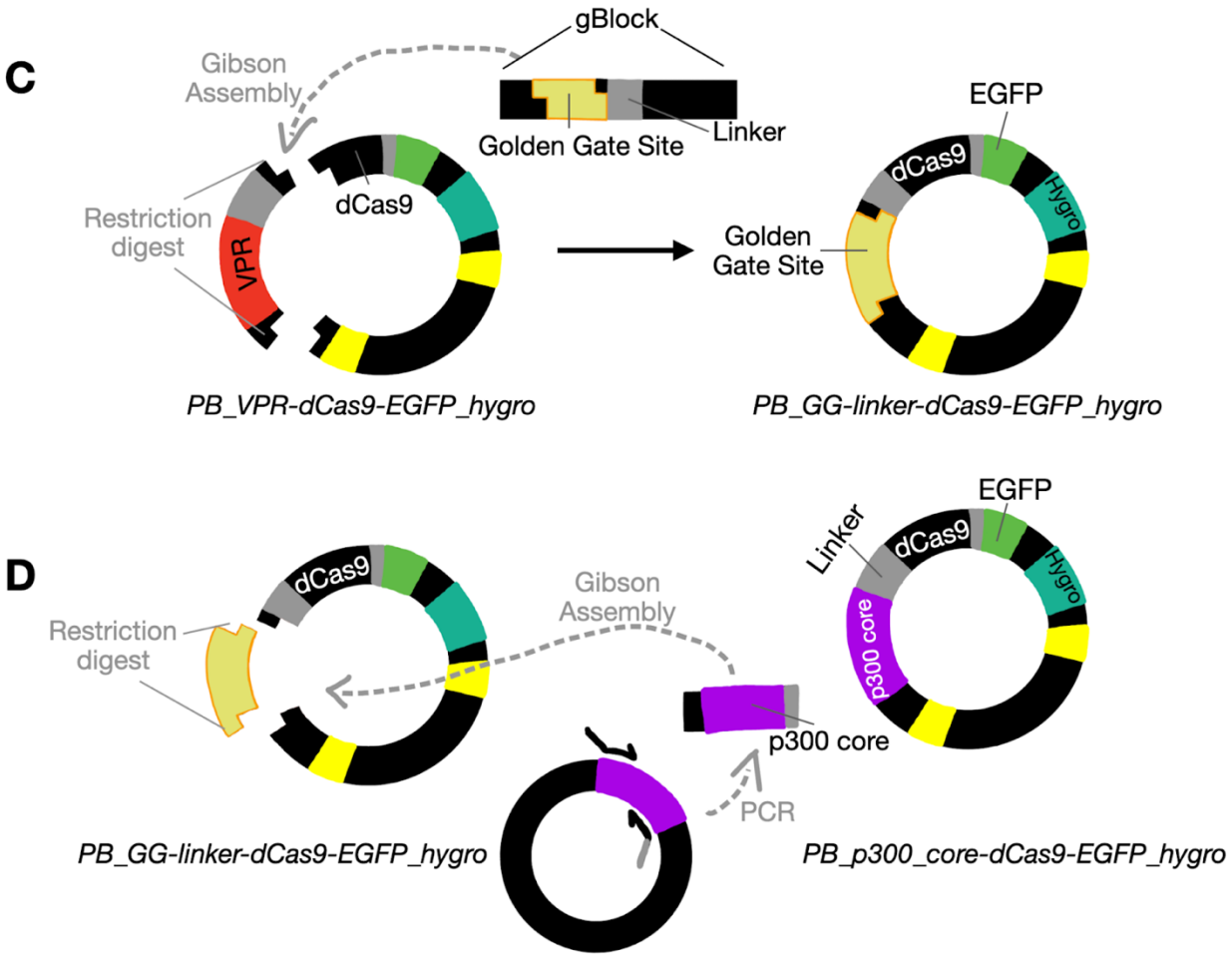

Figure 3. Cloning Procedures for dCas9 fusion protein and gRNA donor constructs (continued).

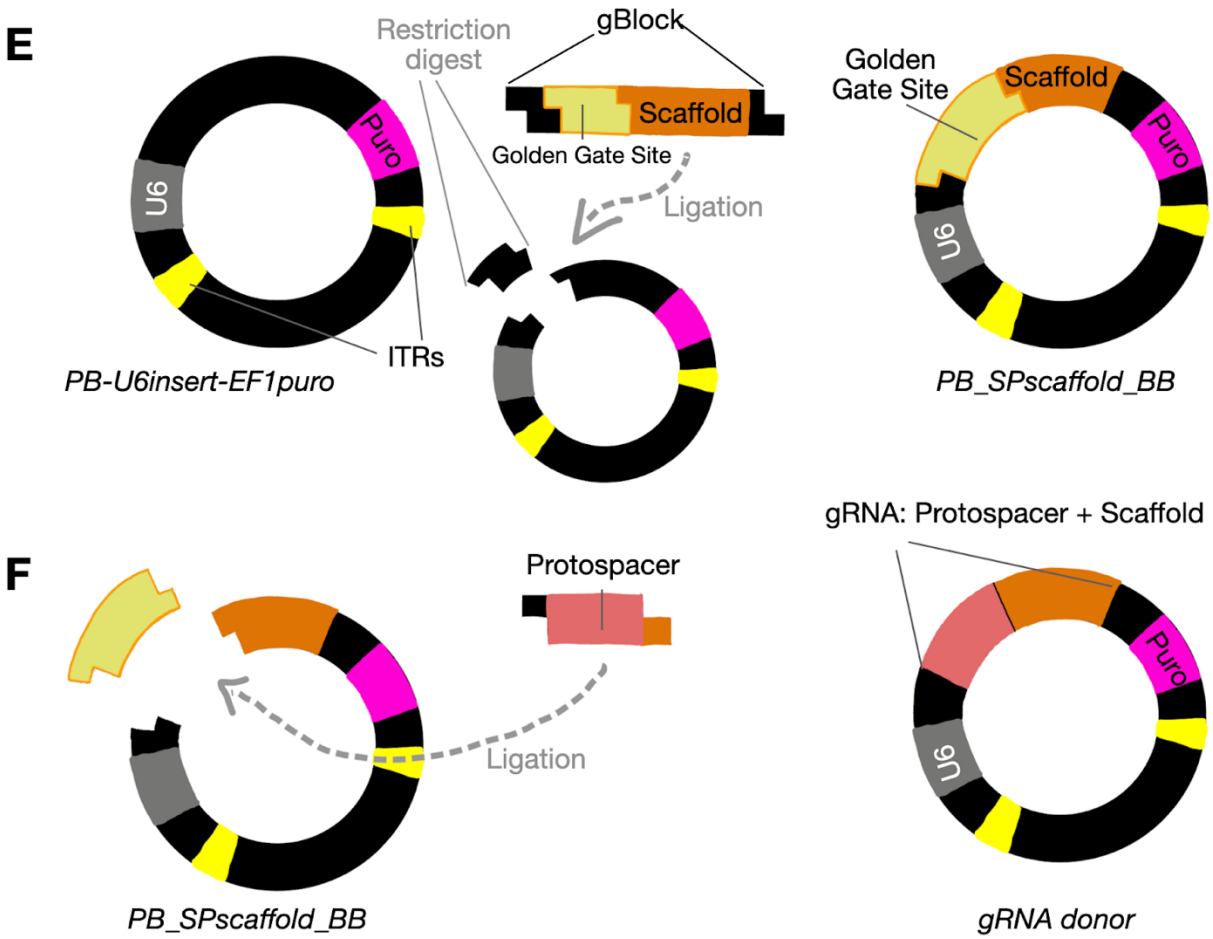

Figure 3. Cloning Procedures for dCas9 fusion protein and gRNA donor constructs (continued).

Chapter 2.2 Normalization of ChIP-seq data to visualize fusion protein directed changes in histone acetylation

Chromatin immunoprecipitation followed by high throughput sequencing or ChIP-seq is a technique that maps genomic positions of chromatin associated proteins or elements such as transcription factors and histone modifications. Briefly, this protocol uses antibodies to capture genomic fragments containing a protein of interest (immunoprecipitation or "IP"), and then sequences the DNA associated with these fragments. Mapping of these sequenced fragments or "tags," (a term I adopted from HOMER http://homer.ucsd.edu/homer/) to a reference genome, can reveal regions of protein enrichment across the genome. Enrichment at a region, in this case, refers to the fraction of tags that map to a region when the chromatin *is* immunoprecipitated over the tags that map to the region when the chromatin is *not* immunoprecipitated. In ChIP terminology, enrichment is IP tags / Input tags.

The global enrichment levels are affected by the IP efficiency of the experiment, or how well the antibody and other steps of the protocol selected for DNA fragments that were actually associated with the protein of interest compared to unassociated "random" pieces of DNA (Bao et al. 2013). High IP efficiency means that your IP samples have a high signal (tags in regions bound the protein of interest) to noise (tags in random regions) ratio. ChIP-seq data can be visualized using different methods depending on the comparisons being made. Local enrichment patterns in a genomic region can be visualized as peaks on the UCSC genome browser (Nassar et al. 2023) or IGV (Robinson et al. 2011), and global comparisons between samples can be made by plotting a scatter plot of tag count values across genomic intervals.

Read depth normalized tag counts of my ChIP-seq experiments displayed stark differences in global enrichment levels (likely due to IP efficiency variations), making it difficult to compare local acetylation changes between samples (**Fig. 4A,E**). Log transformation of the tag counts does not fully correct for this global variation and causes increased relative variability in regions with lower tag counts (**Fig. 4B**). The DESeq2 package contains a variance stabilizing "regularized logarithm" (rlog) transformation, designed to turn heteroskedastic data into more homoskedastic log2 fold change data. Using the empirical Bayes approach, rlog shrinks together the log2 fold change values for the same regions across different samples, especially those with lower tag counts (which experience increased variation after log transformation). This transformation treats each sample like a replicate by ignoring any design matrix, with more samples improving the normalization (**Fig. 4C,D,F**) (Love, Huber, and Anders 2014). This regularization method uses the assumption that for the vast majority of regions, the enrichment levels should be the same. This is appropriate for our samples as the dCas9 fusion protein is only targeted to one region. After performing the rlog transformation on my tag count data, the IP efficiency variations were normalized and direct comparisons between samples could be made. To visualize localization of changes in acetylation enrichment, the rlog normalized tag counts were turned into rlog normalized bigWigs (**Fig. 4F**). Each *treatment condition* bigWig was then subtracted by the appropriate *control condition* bigWig using bigwigCompare from deepTools (**Fig. 4G**).

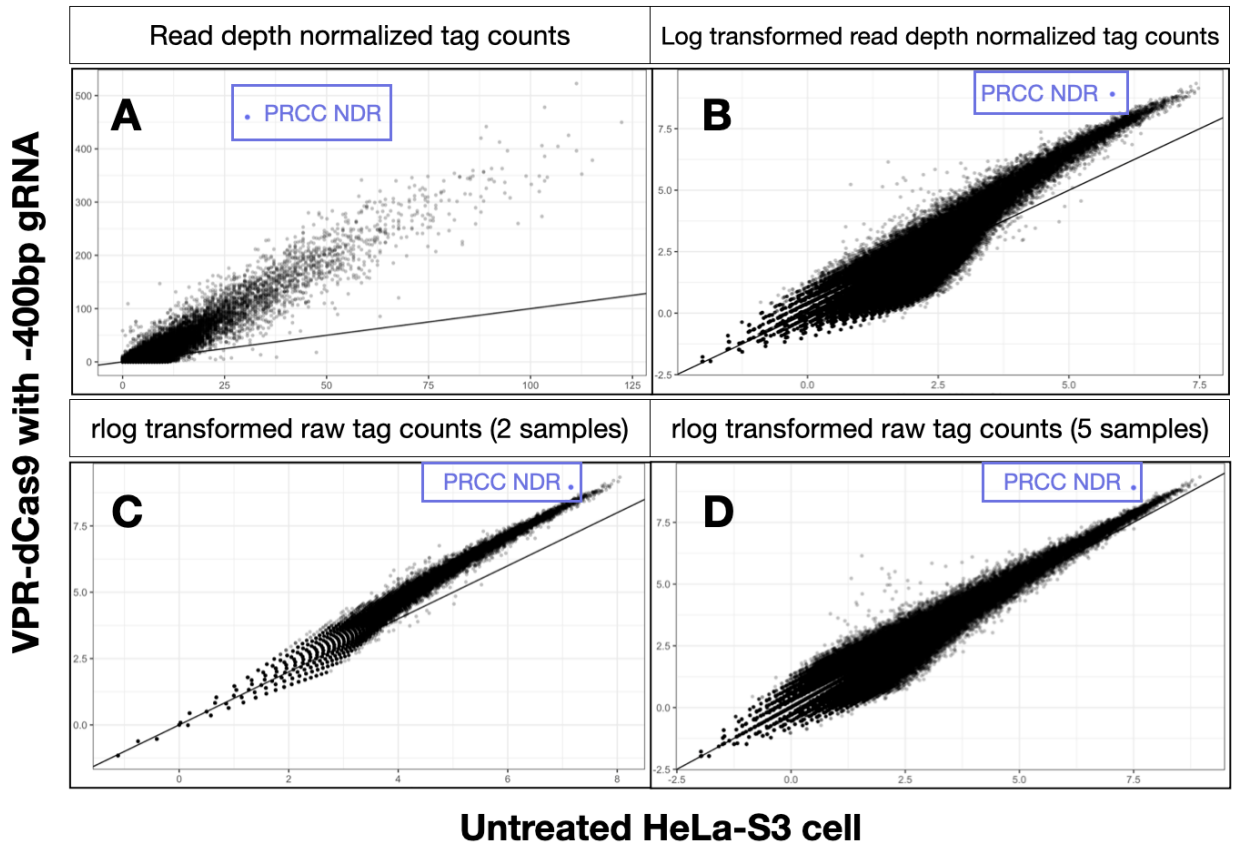

Figure 4. Visualizing changes in local histone acetylation using regularized log transformation to normalize for IP efficiency variation.

A-D) These scatter plots show different methods of normalizing interphase H3K27ac ChIP-seq tag counts to compare treatment sample (VPR-dCas9 with -400bp gRNA) vs untreated control sample. The tag count for the PRCC NDR region is labeled in blue. **A**) Read depth normalization shows a global increase in tag counts for the treatment sample vs the control sample. **B**) Log transformation shows increased variance at lower count values and global increase still present for the treatment sample vs control. **C**) Regularized log transformation calculated using only 2 samples shows smaller variance at lower count values, however global increase of treatment sample still present. **D**) Regularized log transformed tag counts calculated using 5 samples got much better normalization causing treatment and control samples to have similar global tag count values. **E**) Read depth normalized bigWigs show various signal to noise ratios. **F**) Regularized log transformed bigwigs show similar signal to noise ratio between samples. **G**) Treatment rlog transformed bigWigs subtracted by control rlog transformed bigWigs reveals an increase in H3K27ac at the PRCC NDR region for the treatment sample containing VPR-dCas9 and gRNA targeting -400bp from the TSS. View bigWig tracks on UCSC genome browser: https://genome.ucsc.edu/s/emodolo/Fig_4_E%2DG

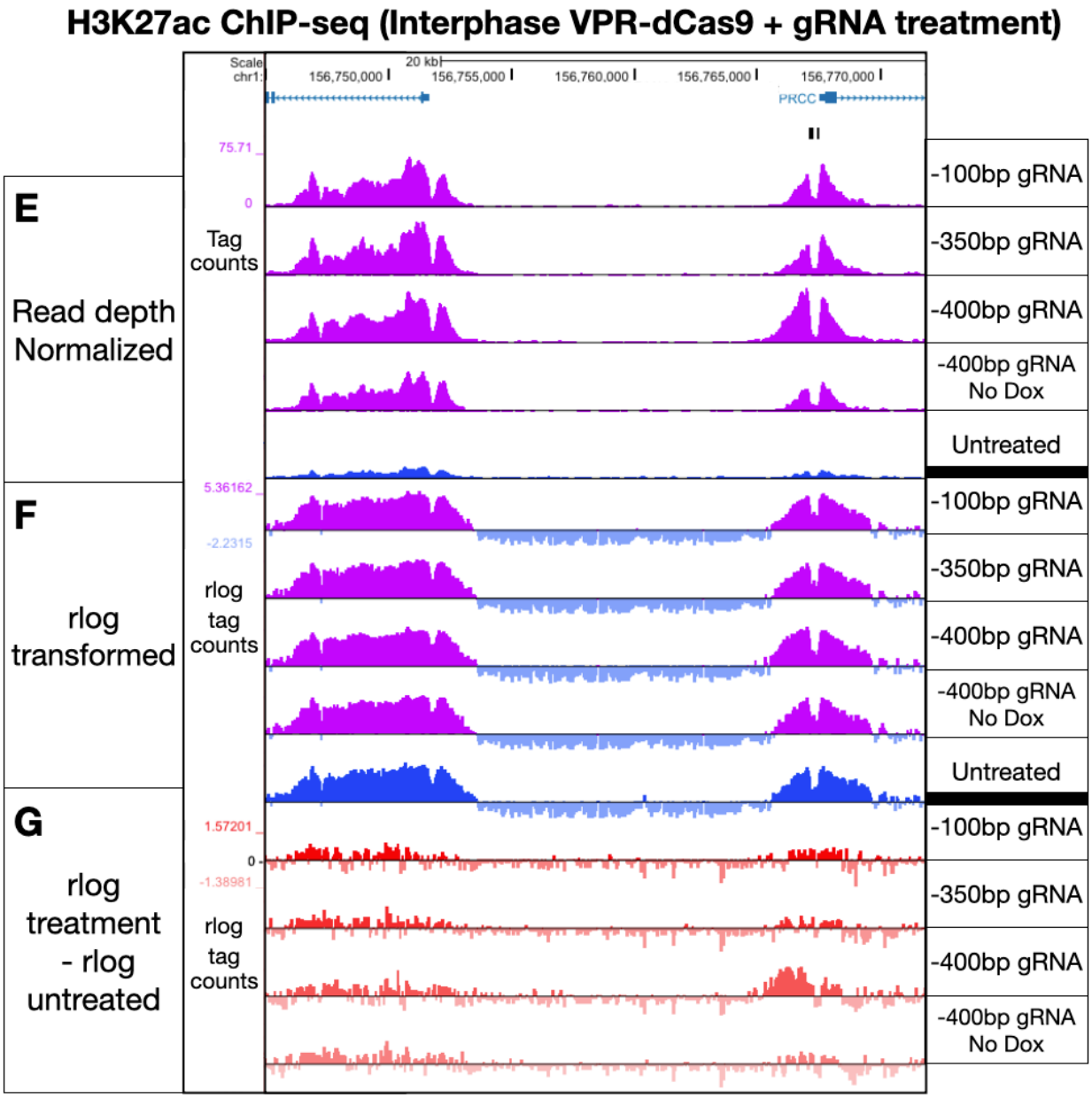

Figure 4. Visualizing changes in local histone acetylation using regularized log transformation to normalize for IP efficiency variation (continued).

Chapter 2.3 ChIP-seq of cell lines harboring dCas9-chimeras shows histone acetylation activity dependent on gRNA target and synchronization condition

The analysis of ChIP-seq results from unsynchronized (interphase) cell lines expressing the VPR-dCas9, showed that H3K27ac acetylation is only increased at the NDR region when the gRNA is targeting -400bp from the TSS (**Fig. 5A**). However, when the cells were synchronized in mitosis, the gRNA targeting -100bp and -400bp from the TSS both showed increase in H3K27ac compared to the negative control (untreated) mitotic HeLa-S3 cells (**Fig. 5B).** Additionally, in the -100bp and -400bp gRNA samples, the peak in acetylation enrichment change is shifted towards the gRNA target position. A similar pattern can be observed for H3K9ac ChIP-seq on VPR-dCas9 cells, where mitotic samples with -100bp and -400bp gRNA targets increase acetylation during mitosis (**Fig. 5D**), however in this case, none of the gRNA targets increase H3K9ac during interphase (**Fig. 5C**). The skewed location of change in acetylation enrichment dependent on the gRNA target is still present in the H3K9ac results.

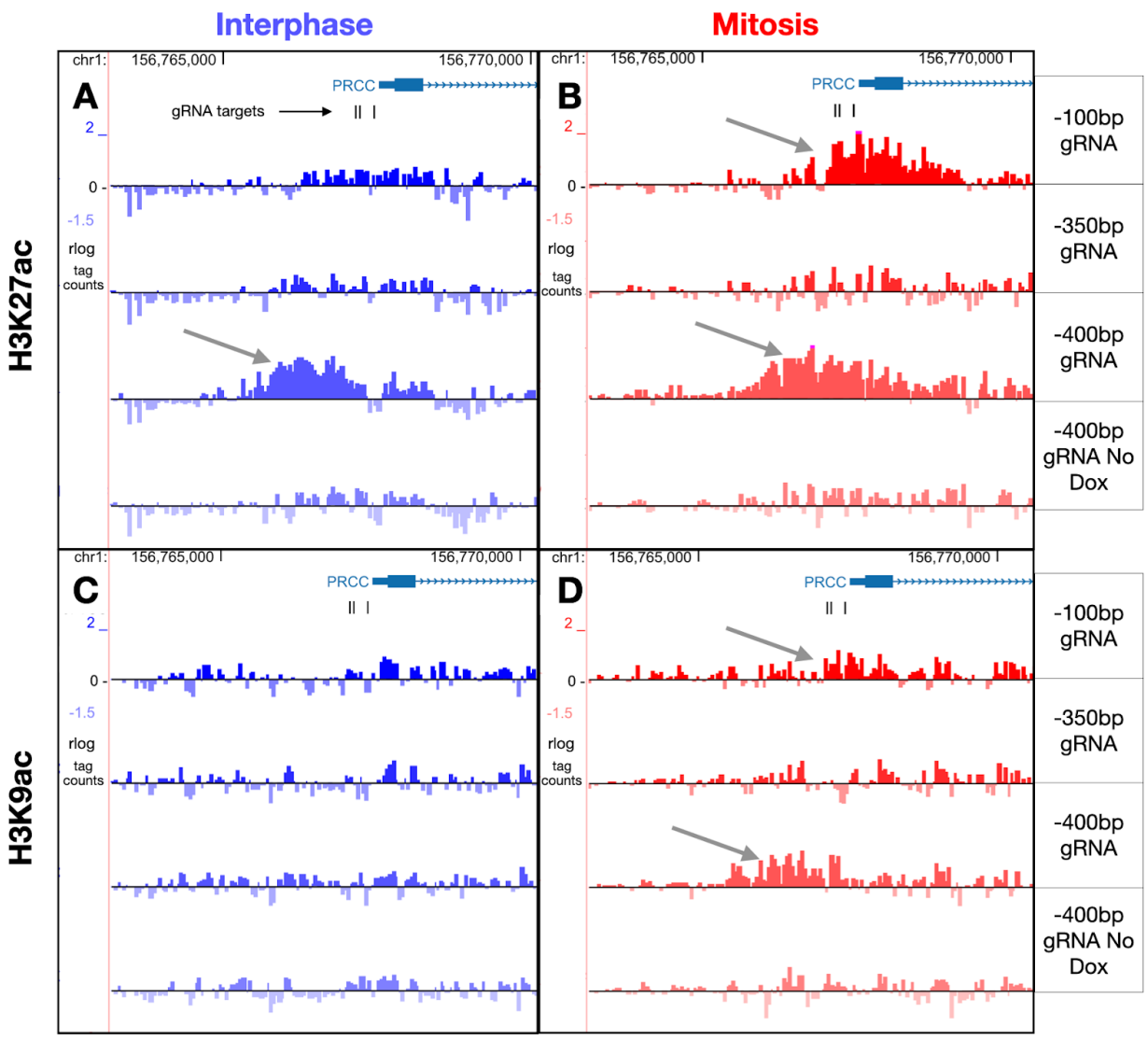

Figure 5. UCSC tracks showing regularized log transformed ChIP-seq tag counts from each treatment (VPR-dCas9 + gRNA targeting PRCC NDR) subtracted by control condition (untreated HeLa-S3).

A) Change in H3K27ac for interphase cells, arrow showing increased acetylation only for the gRNA targeting -400bp from the TSS. **B**) In mitotic cells, H3K27ac is increased when the gRNA targets -100bp and -400bp from the TSS. **C**) H3K9ac is not increased in any condition during interphase. **D**) Mitotic cells show increased H3K9ac when gRNA is targeting -100bp and -400bp from the TSS. View bigWig tracks on UCSC genome browser: https://genome.ucsc.edu/s/emodolo/Fig_5_VPR

ChIP-seq for H3K27ac was performed on the WT and Mut p300 core-dCas9 cell lines; some conditions had technical replicates (a separate ChIP-seq experiment was performed on the same harvested cell population), shown in **Fig. 6** as (replicates). The treatment samples were subtracted by a negative control sample containing the WT fusion protein with a non-targeting gRNA. For the interphase cell lines, none of the WT or Mut conditions for any of the gRNA targets showed an increase in acetylation at the NDR region (**Fig. 6 A,C**). In the mitosis cell lines, only the WT fusion protein targeted to -100bp from the TSS showed an increase in acetylation (**Fig. 6B**).

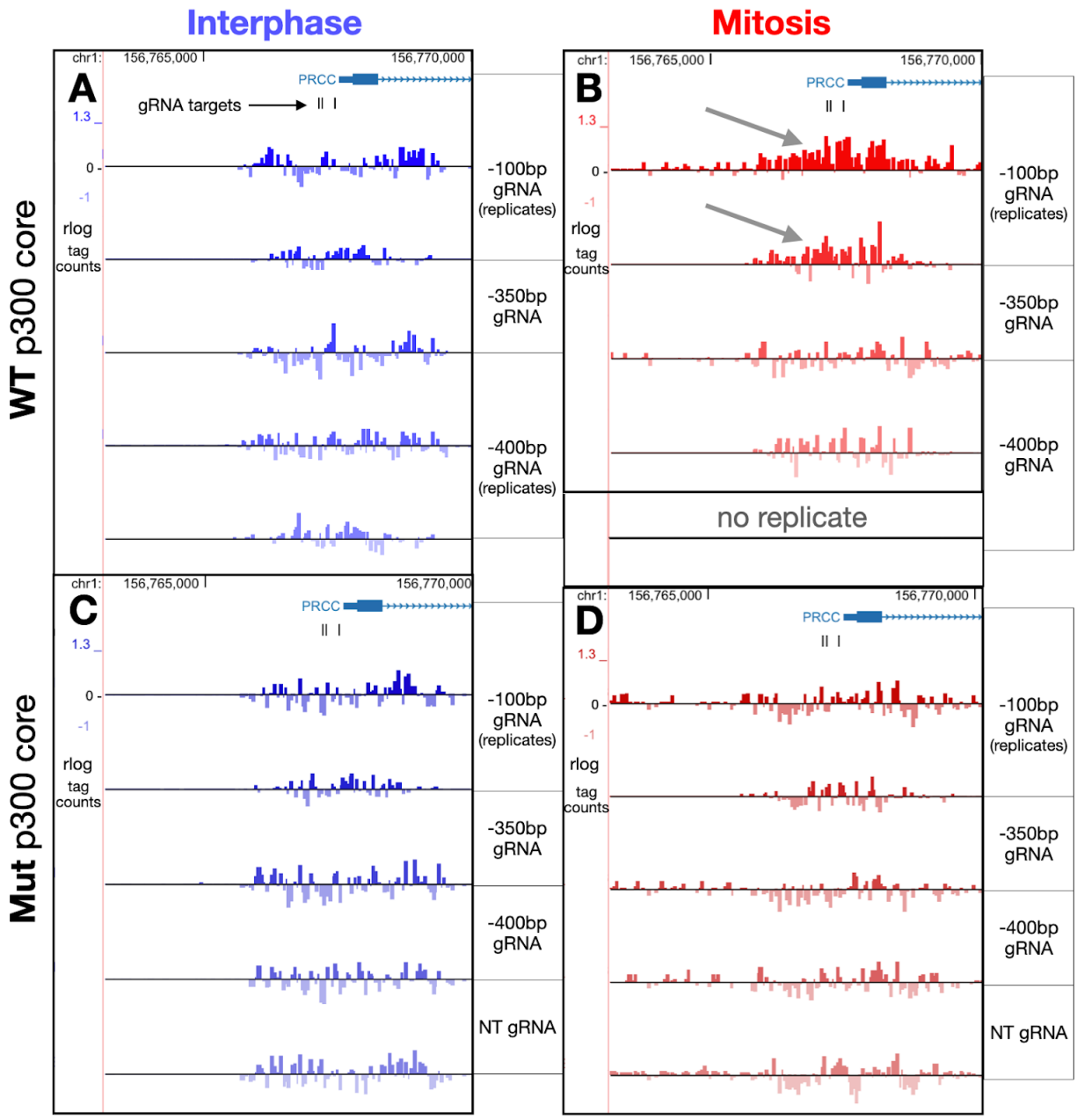

Figure 6. UCSC tracks showing regularized log transformed ChIP-seq tag counts from each treatment (WT/Mut p300 core-dCas9 + gRNA targeting PRCC NDR) subtracted by control condition (WT p300 core-dCas9 + non-targeting gRNA).

A) Interphase cells show no increase in H3K27ac for any gRNA condition. **B)** Mitotic cells show increased H3K27ac only when the gRNA targets -100bp from the TSS. **C-D)** Interphase and mitosis cells both show no increase in acetylation in any condition for the mutant p300 core-dCas9 cell lines. View bigWigs tracks on UCSC genome browser: https://genome.ucsc.edu/s/emodolo/Fig_6_p300

Chapter 3 DISCUSSION

Chapter 3.1 Conclusions and possible explanations

After analysis of the ChIP-seq data from my dCas9 fusion protein cell lines, we can make some preliminary conclusions about the feasibility of using a CRISPR-dCas9 system to interrogate our mitotic bookmarking hypothesis. Our hypothesis states that the histone acetylation condition of the nucleosome occupying the NDR of most gene promoters during mitosis bookmarks these genes, affecting their post-mitotic reactivation kinetics. To test this hypothesis, we will need to experimentally perturb the bookmark specifically in mitosis to later measure the impact on reactivation kinetics. We are utilizing fusion proteins that cause acetylation to perturb the deacetylated nucleosomes in the NDR of most genes during mitosis (Group 2 genes). We saw that when targeted to -100bp from the TSS of a test gene: PRCC, our wild type p300 core-dCas9 and VPR-dCas9 fusion proteins are able to robustly increase acetylation of the region. Note: Likely due to either suboptimal nucleosome positioning affecting the dCas9 binding (Handelmann et al. 2023), or the poor off target score of the protospacer, the gRNA targeting -350bp from the TSS showed no effect on acetylation in either interphase or mitosis, for both the VPR-dCas9 and WT p300 core-dCas9.

While perturbation of the NDR acetylation pattern is achieved, the effect range of this acetylation increase is not limited to the nucleosome occupying the NDR, with some increased enrichment seen in the nucleosomes surrounding the NDR as well. This is a limitation of the dCas9 fusion protein system and further research will be necessary to determine if nucleosome specific acetylation is attainable. Additionally, possible off-target binding of the fusion protein is another limitation observed in our system. Future experiments will take further precautions in the design

of gRNA protospacers, using tools such as Cas-OFFinder (http://www.rgenome.net/cas-offinder/) to predict and limit this off-target activity.

The retention of the dCas9 binding at the NDR during interphase and steric inhibition of transcriptional machinery could also affect the reactivation kinetics observed for our targeted genes. The mutant p300 core fusion protein would be used to control for possible confounding effects that accompanies the targeting of a dCas9 fusion protein to the region.

Another requirement to test the mitotic bookmarking hypothesis is that the system must have a method for phase-controlled perturbation, altering the acetylation state only in mitosis. Somewhat surprisingly, when targeting -100bp from the TSS, all fusion proteins increased acetylation only during mitosis. The cause of this observation is currently being investigated. A possible explanation could be that the dCas9 fusion protein is binding to the NDR during interphase, however the effector cannot reach a nucleosome to acetylate. Then during mitosis, when a nucleosome enters the NDR, this repositioning could provide the nucleosome proximity necessary for fusion protein catalyzed acetylation. Future experiments with guides targeting multiple genes and loci up and downstream of the NDR could help explain this observation.

In **Figure 5A** and **5C**, we see that the VPR-dCas9 with the gRNA targeting -400bp from the TSS increases H3K27ac but not H3K9ac during interphase. However, this fusion protein and guide target increases both H3K27ac and H3K9ac in mitosis (**Fig 5B,D**). One reason for this observation could be possible saturation of H3K9ac in interphase making it difficult to increase levels of this acetylation mark. When the global decrease in histone acetylation occurs in mitosis, it may free up histone residues for our fusion protein to cause acetylation. Future experiments with spike-in normalized ChIP-seq could help illuminate the cause of this mitotic specific increase in acetylation.

Overall, the CRISPR-dCas9 system is not without its limitations, however the data collected in this study suggests that this system can cause directed local histone acetylation changes specifically in mitosis, making it a feasible option to experimentally test our hypothesized mitotic bookmark.

Chapter 3.2 Future directions

There are many future directions we are excited to take this project. We are currently working to get capped-small RNA-seq (csRNA-seq) (Duttke et al. 2019) data from the mitotic and interphase VPR-dCas9 fusion protein cell lines, to inspect any effects on nascent transcription levels and transcription initiation sites. We will continue to gather csRNA-seq data from our wild type and mutant p300 core-dCas9 cell lines as well, to measure any effects that the fusion protein may have caused on transcription initiation in interphase and mitotic cell populations.

Using a library of gRNA protospacers, we plan to create cell lines with the fusion protein targeted to a specified distance from the TSS for multiple genes (example: a cell line with gRNAs targeting -100bp from the TSS of 20 genes, and a different cell line with gRNAs targeting -400bp from the TSS of those same 20 genes) (**Fig. 7**). We could then study the acetylation activity of the fusion protein at multiple genomic contexts and genes Groups with just a few ChIP samples, while still allowing for the distinction between chimera activity when targeted to different loci within the NDR.

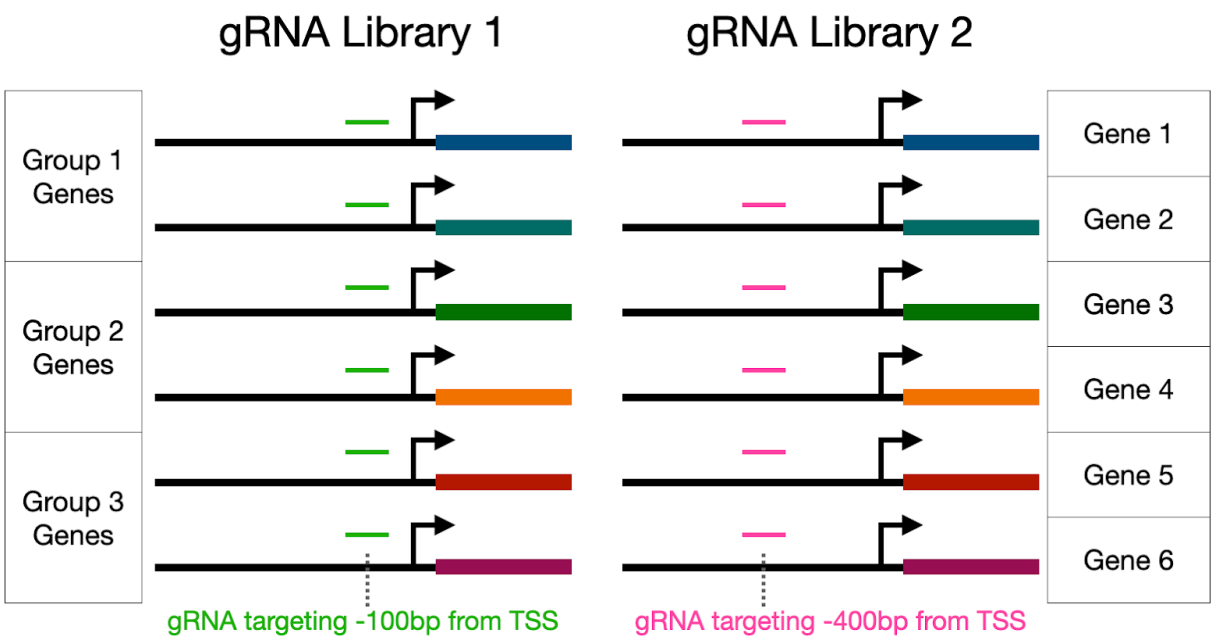

Figure 7. Schematic representation of a gRNA library targeting a fixed distance from the TSS of multiple genes.

REFERENCES

Andrews, Simon. 2010. “Babraham Bioinformatics - FastQC A Quality Control Tool for High Throughput Sequence Data.” 2010. https://www.bioinformatics.babraham.ac.uk/projects/fastqc/.

Bai, Lu, Gilles Charvin, Eric Siggia, and Frederick Cross. 2010. “Nucleosome Depleted Regions in Cell-Cycle-Regulated Promoters Ensure Reliable Gene Expression in Every Cell Cycle.” Developmental Cell 18 (4): 544–55. https://doi.org/10.1016/j.devcel.2010.02.007.

Bao, Yanchun, Veronica Vinciotti, Ernst Wit, and Peter AC ’t Hoen. 2013. “Accounting for Immunoprecipitation Efficiencies in the Statistical Analysis of ChIP-Seq Data.” BMC Bioinformatics 14 (May):169. https://doi.org/10.1186/1471-2105-14-169.

Bellec, Maëlle, Jérémy Dufourt, George Hunt, Hélène Lenden-Hasse, Antonio Trullo, Amal Zine El Aabidine, Marie Lamarque, Marissa M. Gaskill, Heloïse Faure-Gautron, Mattias Mannervik, Melissa M. Harrison, Jean-Christophe Andrau, Cyril Favard, Ovidiu Radulescu, and Mounia Lagha. 2022. “The Control of Transcriptional Memory by Stable Mitotic Bookmarking.” Nature Communications 13 (1): 1176. https://doi.org/10.1038/s41467-022-28855-y.

Bellec, Maelle, Ovidiu Radulescu, and Mounia Lagha. 2018. “Remembering the Past: Mitotic Bookmarking in a Developing Embryo.” Current Opinion in Systems Biology, • Big data acquisition and analysis • Development and differentiation, 11 (October):41–49. https://doi.org/10.1016/j.coisb.2018.08.003.

Bolger, Anthony M., Marc Lohse, and Bjoern Usadel. 2014. “Trimmomatic: A Flexible Trimmer for Illumina Sequence Data.” Bioinformatics 30 (15): 2114–20. https://doi.org/10.1093/bioinformatics/btu170.

Chen, Jihong, and Qiao Li. 2011. “Life and Death of Transcriptional Co-Activator P300.” *Epigenetics* 6 (8): 957–61. https://doi.org/10.4161/epi.6.8.16065.

Delvecchio, Manuela, Jonathan Gaucher, Carmen Aguilar-Gurrieri, Esther Ortega, and Daniel Panne. 2013. “Structure of the P300 Catalytic Core and Implications for Chromatin Targeting and HAT Regulation.” Nature Structural & Molecular Biology 20 (9): 1040–46. https://doi.org/10.1038/nsmb.2642.

Duttke, Sascha H., Max W. Chang, Sven Heinz, and Christopher Benner. 2019. “Identification and Dynamic Quantification of Regulatory Elements Using Total RNA.” Genome Research 29 (11): 1836–46. https://doi.org/10.1101/gr.253492.119.

Engler, Carola, and Sylvestre Marillonnet. 2014. “Golden Gate Cloning.” Methods in Molecular Biology (Clifton, N.J.) 1116:119–31. https://doi.org/10.1007/978-1-62703-764-8_9.

Festuccia, Nicola, Inma Gonzalez, Nick Owens, and Pablo Navarro. 2017. “Mitotic Bookmarking in Development and Stem Cells.” Development 144 (20): 3633–45. https://doi.org/10.1242/dev.146522.

Fuentes, Daniel R, Tomek Swigut, and Joanna Wysocka. 2018. “Systematic Perturbation of Retroviral LTRs Reveals Widespread Long-Range Effects on Human Gene Regulation.” Edited by Edith Heard and Detlef Weigel. eLife 7 (August):e35989. https://doi.org/10.7554/eLife.35989.

Genga, Ryan M., Nicola A. Kearns, and René Maehr. 2016. “Controlling Transcription in Human Pluripotent Stem Cells Using CRISPR-Effectors.” Methods, Human Pluripotent Stem Cells, 101 (May):36–42. https://doi.org/10.1016/j.ymeth.2015.10.014.

Gibson, Daniel G., Lei Young, Ray-Yuan Chuang, J. Craig Venter, Clyde A. Hutchison, and Hamilton O. Smith. 2009. “Enzymatic Assembly of DNA Molecules up to Several Hundred Kilobases.” Nature Methods 6 (5): 343–45. https://doi.org/10.1038/nmeth.1318.

Handelmann, Christopher R, Maria Tsompana, Ram Samudrala, and Michael J Buck. 2023. “The Impact of Nucleosome Structure on CRISPR/Cas9 Fidelity.” Nucleic Acids Research 51 (5): 2333–44. https://doi.org/10.1093/nar/gkad021.

Hart, Traver, H Kiyomi Komori, Sarah LaMere, Katie Podshivalova, and Daniel R Salomon. 2013. “Finding the Active Genes in Deep RNA-Seq Gene Expression Studies.” BMC Genomics 14 (November):778. https://doi.org/10.1186/1471-2164-14-778.

Hassan, A. H., K. E. Neely, and J. L. Workman. 2001. “Histone Acetyltransferase Complexes Stabilize Swi/Snf Binding to Promoter Nucleosomes.” Cell 104 (6): 817–27. https://doi.org/10.1016/s0092-8674(01)00279-3.

Hassan, Ahmed H., Philippe Prochasson, Kristen E. Neely, Scott C. Galasinski, Mark Chandy, Michael J. Carrozza, and Jerry L. Workman. 2002. “Function and Selectivity of Bromodomains in Anchoring Chromatin-Modifying Complexes to Promoter Nucleosomes.” Cell 111 (3): 369–79. https://doi.org/10.1016/s0092-8674(02)01005-x.

Heinz, Sven, Christopher Benner, Nathanael Spann, Eric Bertolino, Yin C. Lin, Peter Laslo, Jason X. Cheng, Cornelis Murre, Harinder Singh, and Christopher K. Glass. 2010. “Simple Combinations of Lineage-Determining Transcription Factors Prime Cis-Regulatory Elements Required for Macrophage and B Cell Identities.” Molecular Cell 38 (4): 576–89. https://doi.org/10.1016/j.molcel.2010.05.004.

Hilton, Isaac B., Anthony M. D’Ippolito, Christopher M. Vockley, Pratiksha I. Thakore, Gregory E. Crawford, Timothy E. Reddy, and Charles A. Gersbach. 2015. “Epigenome Editing by a CRISPR-Cas9-Based Acetyltransferase Activates Genes from Promoters and Enhancers.” Nature Biotechnology 33 (5): 510–17. https://doi.org/10.1038/nbt.3199.

Javasky, Elisheva, Inbal Shamir, Shashi Gandhi, Shawn Egri, Oded Sandler, Scott B. Rothbart, Noam Kaplan, Jacob D. Jaffe, Alon Goren, and Itamar Simon. 2018. “Study of Mitotic Chromatin Supports a Model of Bookmarking by Histone Modifications and Reveals

Nucleosome Deposition Patterns." Genome Research 28 (10): 1455–66. https://doi.org/10.1101/gr.230300.117.

Kampmann, Martin. 2018. "CRISPRi and CRISPRa Screens in Mammalian Cells for Precision Biology and Medicine." ACS Chemical Biology 13 (2): 406–16. https://doi.org/10.1021/acschembio.7b00657.

Karlson, Chou Khai Soong, Siti Nurfadhlina Mohd-Noor, Nadja Nolte, and Boon Chin Tan. 2021. "CRISPR/dCas9-Based Systems: Mechanisms and Applications in Plant Sciences." Plants 10 (10): 2055. https://doi.org/10.3390/plants10102055.

Kelly, Theresa K., Tina Branscombe Miranda, Gangning Liang, Benjamin P. Berman, Joy C. Lin, Amos Tanay, and Peter A. Jones. 2010. "H2A.Z Maintenance During Mitosis Reveals Nucleosome Shifting on Mitotically Silenced Genes." Molecular Cell 39 (6): 901–11. https://doi.org/10.1016/j.molcel.2010.08.026.

Kent, W. J., A. S. Zweig, G. Barber, A. S. Hinrichs, and D. Karolchik. 2010. "BigWig and BigBed: Enabling Browsing of Large Distributed Datasets." Bioinformatics 26 (17): 2204–7. https://doi.org/10.1093/bioinformatics/btq351.

Li, Heng, and Richard Durbin. 2009. "Fast and Accurate Short Read Alignment with Burrows–Wheeler Transform." Bioinformatics 25 (14): 1754–60. https://doi.org/10.1093/bioinformatics/btp324.

Liang, Kaiwei, Ashley R. Woodfin, Brian D. Slaughter, Jay R. Unruh, Andrew C. Box, Ryan A. Rickels, Xin Gao, Jeffrey S. Haug, Sue L. Jaspersen, and Ali Shilatifard. 2015. "Mitotic Transcriptional Activation: Clearance of Actively Engaged Pol II via Transcriptional Elongation Control in Mitosis." Molecular Cell 60 (3): 435–45. https://doi.org/10.1016/j.molcel.2015.09.021.

Liu, Yiyuan, Bobbie Pelham-Webb, Dafne Campigli Di Giammartino, Jiexi Li, Daleum Kim, Katsuhiro Kita, Nestor Saiz, Vidur Garg, Ashley Doane, Paraskevi Giannakakou, Anna-Katerina Hadjantonakis, Olivier Elemento, and Effie Apostolou. 2017. "Widespread Mitotic Bookmarking by Histone Marks and Transcription Factors in Pluripotent Stem Cells." Cell Reports 19 (7): 1283–93. https://doi.org/10.1016/j.celrep.2017.04.067.

Love, Michael I., Wolfgang Huber, and Simon Anders. 2014. "Moderated Estimation of Fold Change and Dispersion for RNA-Seq Data with DESeq2." Genome Biology 15 (12): 550. https://doi.org/10.1186/s13059-014-0550-8.

Manning, E. Tory, Tsuyoshi Ikehara, Takashi Ito, James T. Kadonaga, and W. Lee Kraus. 2001. "P300 Forms a Stable, Template-Committed Complex with Chromatin: Role for the Bromodomain." Molecular and Cellular Biology 21 (12): 3876–87. https://doi.org/10.1128/MCB.21.12.3876-3887.2001.

Nassar, Luis R., Galt P. Barber, Anna Benet-Pagès, Jonathan Casper, Hiram Clawson, Mark Diekhans, Clay Fischer, Jairo Navarro Gonzalez, Angie S. Hinrichs, Brian T. Lee, Christopher M. Lee, Pranav Muthuraman, Beagan Nguy, Tiana Pereira, Parisa Nejad, Gerardo Perez, Brian J. Raney, Daniel Schmelter, Matthew L. Speir, Brittney D. Wick, Ann S. Zweig, David Haussler, Robert M. Kuhn, Maximilian Haeussler, and W. James Kent. 2023. "The UCSC Genome Browser Database: 2023 Update." Nucleic Acids Research 51 (D1): D1188–95. https://doi.org/10.1093/nar/gkac1072.

Naumova, Natalia, Maxim Imakaev, Geoffrey Fudenberg, Ye Zhan, Bryan R. Lajoie, Leonid A. Mirny, and Job Dekker. 2013. "Organization of the Mitotic Chromosome." Science (New York, N.Y.) 342 (6161): 948–53. https://doi.org/10.1126/science.1236083.

Palozola, Katherine C., Greg Donahue, Hong Liu, Gregory R. Grant, Justin S. Becker, Allison Cote, Hongtao Yu, Arjun Raj, and Kenneth S. Zaret. 2017. "Mitotic Transcription and Waves of Gene Reactivation during Mitotic Exit." Science 358 (6359): 119–22. https://doi.org/10.1126/science.aal4671.

Palozola, Katherine C., Jonathan Lerner, and Kenneth S. Zaret. 2019. "A Changing Paradigm of Transcriptional Memory Propagation through Mitosis." Nature Reviews. Molecular Cell Biology 20 (1): 55–64. https://doi.org/10.1038/s41580-018-0077-z.

Park, Sangho, Maria A. Martinez-Yamout, H. Jane Dyson, and Peter E. Wright. 2013. "The CH2 Domain of CBP/P300 Is a Novel Zinc Finger." FEBS Letters 587 (16): 2506–11. https://doi.org/10.1016/j.febslet.2013.06.051.

Parsons, G G, and C A Spencer. 1997. "Mitotic Repression of RNA Polymerase II Transcription Is Accompanied by Release of Transcription Elongation Complexes." Molecular and Cellular Biology 17 (10): 5791–5802.

Prasanth, Kannanganattu V., Paula A. Sacco-Bubulya, Supriya G. Prasanth, and David L. Spector. 2003. "Sequential Entry of Components of Gene Expression Machinery into Daughter Nuclei." Molecular Biology of the Cell 14 (3): 1043–57. https://doi.org/10.1091/mbc.E02-10-0669.

Qi, Lei S., Matthew H. Larson, Luke A. Gilbert, Jennifer A. Doudna, Jonathan S. Weissman, Adam P. Arkin, and Wendell A. Lim. 2013. "Repurposing CRISPR as an RNA-Guided Platform for Sequence-Specific Control of Gene Expression." Cell 152 (5): 1173–83. https://doi.org/10.1016/j.cell.2013.02.022.

Raccaud, Mahé, and David M. Suter. 2018. "Transcription Factor Retention on Mitotic Chromosomes: Regulatory Mechanisms and Impact on Cell Fate Decisions." FEBS Letters 592 (6): 878–87. https://doi.org/10.1002/1873-3468.12828.

Robinson, James T., Helga Thorvaldsdóttir, Wendy Winckler, Mitchell Guttman, Eric S. Lander, Gad Getz, and Jill P. Mesirov. 2011. "Integrative Genomics Viewer." Nature Biotechnology 29 (1): 24–26. https://doi.org/10.1038/nbt.1754.

Skoufias, Dimitrios A., Salvatore DeBonis, Yasmina Saoudi, Luc Lebeau, Isabelle Crevel, Robert Cross, Richard H. Wade, David Hackney, and Frank Kozielski. 2006. “S-Trityl-L-Cysteine Is a Reversible, Tight Binding Inhibitor of the Human Kinesin Eg5 That Specifically Blocks Mitotic Progression*.” Journal of Biological Chemistry 281 (26): 17559–69. https://doi.org/10.1074/jbc.M511735200.

Struhl, Kevin, and Eran Segal. 2013. “Determinants of Nucleosome Positioning.” Nature Structural & Molecular Biology 20 (3): 267–73. https://doi.org/10.1038/nsmb.2506.

Swygert, Sarah G., and Craig L. Peterson. 2014. “Chromatin Dynamics: Interplay between Remodeling Enzymes and Histone Modifications.” Biochimica et Biophysica Acta (BBA) - Gene Regulatory Mechanisms, Molecular mechanisms of histone modification function, 1839 (8): 728–36. https://doi.org/10.1016/j.bbagrm.2014.02.013.

Texari, Lorane, Nathanael J. Spann, Ty D. Troutman, Mashito Sakai, Jason S. Seidman, and Sven Heinz. 2021. “An Optimized Protocol for Rapid, Sensitive and Robust on-Bead ChIP-Seq from Primary Cells.” STAR Protocols 2 (1): 100358. https://doi.org/10.1016/j.xpro.2021.100358.

Wang, Fangwei, and Jonathan M. G. Higgins. 2013. “Histone Modifications and Mitosis: Countermarks, Landmarks, and Bookmarks.” Trends in Cell Biology 23 (4): 175–84. https://doi.org/10.1016/j.tcb.2012.11.005.

Whitfield, Michael L., Gavin Sherlock, Alok J. Saldanha, John I. Murray, Catherine A. Ball, Karen E. Alexander, John C. Matese, Charles M. Perou, Myra M. Hurt, Patrick O. Brown, and David Botstein. 2002. “Identification of Genes Periodically Expressed in the Human Cell Cycle and Their Expression in Tumors.” Molecular Biology of the Cell 13 (6): 1977–2000. https://doi.org/10.1091/mbc.02-02-0030.

Zaret, Kenneth S. 2014. “Genome Reactivation after the Silence in Mitosis: Recapitulating Mechanisms of Development?” Developmental Cell 29 (2): 132–34. https://doi.org/10.1016/j.devcel.2014.04.019.

Zhao, Rui, Tetsuya Nakamura, Yu Fu, Zsolt Lazar, and David L. Spector. 2011. “Gene Bookmarking Accelerates the Kinetics of Post-Mitotic Transcriptional Re-Activation.” Nature Cell Biology 13 (11): 1295–1304. https://doi.org/10.1038/ncb2341.

Zhao, Shuang, Enze Jiang, Shuangshuang Chen, Yuan Gu, Anna Junjie Shangguan, Tangfeng Lv, Liguo Luo, and Zhenghong Yu. 2016. “PiggyBac Transposon Vectors: The Tools of the Human Gene Encoding.” Translational Lung Cancer Research 5 (1): 120–25. https://doi.org/10.3978/j.issn.2218-6751.2016.01.05.